

# Groups in the Millennium Simulation and in SDSS DR7

P. Nurmi<sup>1\*</sup>, P. Heinämäki<sup>1</sup>, T. Sepp<sup>2,5</sup>, E. Tago<sup>2</sup>, E. Saar<sup>2,4</sup>, M. Gramann<sup>2</sup>,  
M. Einasto<sup>2</sup>, E. Tempel<sup>2,3</sup> and J. Einasto<sup>2,4,6</sup>

<sup>1</sup>*Tuorla Observatory, Department of Physics and Astronomy, University of Turku, Väisäläntie 20, FI-21500 Piikkiö, Finland*

<sup>2</sup>*Tartu Observatory, Tõravere, Tartumaa, 61602 Estonia*

<sup>3</sup>*National Institute of Chemical Physics and Biophysics, Tallinn 10143, Estonia*

<sup>4</sup>*Estonian Academy of Sciences, EE-10130 Tallinn, Estonia*

<sup>5</sup>*Institute of Physics, University of Tartu, Estonia*

<sup>6</sup>*ICRANet, Piazza della Repubblica 10, 65122 Pescara, Italy*

Accepted - . Received -; in original form -

## ABSTRACT

The Millennium N-body simulation and SDSS DR7 galaxy and galaxy group catalogues are compared to study the properties of galaxy groups and the distribution of galaxies in groups. We construct mock galaxy group catalogues for a Millennium semi-analytical galaxy catalogue by using the same friends-of-friends method, which was used by Tago et al. (2010) to analyse the SDSS data. We analyse in detail the group luminosities, group richnesses, virial radii, sizes of groups and their rms velocities for four volume-limited samples from observations and simulations. Our results show that the spatial densities of groups agree within one order of magnitude in all samples with a rather good agreement between the mock catalogues and observations. All group property distributions have similar shapes and amplitudes for richer groups. For galaxy pairs and small groups the group properties for observations and simulations are clearly different. In addition, the spatial distribution of galaxies in small groups is different: at the outskirts of the groups the galaxy number distributions do not agree, although the agreement is relatively good in the inner regions. Differences in the distributions are mainly due to the observational limitations in the SDSS sample and to the problems in the semi-analytical methods that produce too compact and luminous groups.

**Key words:** methods: numerical – methods: statistical – galaxies: clusters: general – cosmology: miscellaneous – large-scale structure of Universe

## 1 INTRODUCTION

In the hierarchical picture of galaxy formation, galaxies form by baryon cooling within dark matter (DM) haloes; after that they cluster gravitationally to form galaxy groups and clusters of galaxies. During this process several hydrodynamical (e.g., ram pressure stripping, viscous stripping, strangulation) and gravitational (tidal interaction between galaxies, galaxy merging) processes together lead to virialized groups and clusters. At the same time these processes modify galaxy morphologies in dense environments and establish the well known morphology-density relation (Einasto et al. 1974, Dressler 1980, Potsman & Geller 1984). In the hierarchical picture, groups and clusters of galaxies are generally assumed to be systems embedded in an extended dark matter halo whereas satellite galaxies themselves reside in

dark matter subhaloes. Simulations strongly support this picture, although still some problems related to the smallest DM subhaloes remain (e.g., Guo et al. 2011, Klypin et al. 2011).

Recent numerical and analytical studies of the cluster scale DM haloes show that cluster abundances (Press & Schechter 1974, Jenkins et al. 2001 and Sheth & Tormen 1999) and two-point correlation functions agree well (Springel et al. 2005, Conroy, Wechsler and Kravtsov 2006) with observations. When the galaxy formation physics, incorporated in smoothed-particle hydrodynamics (SPH) simulations, has been taken into account, good agreement with observed galaxy clustering is obtained (e.g., Weinberg et al. 2004 and Maller et al. 2006). Summarizing, the agreement between the observational data and theoretical studies of galaxy clusters is relatively good, but is the agreement as good for the galaxy group scale?

From observations we know that most galaxies are situ-

\* pasnurmi@utu.fi

ated in galaxy groups (e.g. Geller & Huchra 1983, Mulchaey 2000, Eke et al. 2005, Karachentsev 2005), meaning that group environment has an important role in structure formation and galaxy evolution. Different group catalogues can be compiled, even from the same data set, by using different algorithms. The most widely used method is the friends-of-friends (FOF) algorithm used already by Geller & Huchra (1983). Different implementations of this algorithm have been used, e.g., for the following group catalogues: Tucker et al. (2000), Allam & Tucker (2000), Blanton et al. (2005), Berlind et al. (2006), Yang et al. (2007), Tago et al. (2008), Tempel et al. (2012), Muñoz-Cuartas & Müller (2012) and Wen et al. (2012).

From observations we know that galaxy clusters and galaxy groups are not distinct classes of objects. This can be seen in a continuous richness distribution from galaxy pairs to rich groups and clusters in observations (Berlind et al. 2006). Indeed, in many ways groups can be viewed as scaled-down versions of clusters; e.g., many X-ray scaling relations extend from clusters to groups although the scatter in the correlations increases towards smaller systems (Mulchaey 2000, Sun et al. 2009, Eckmiller, Hudson and Reiprich 2011). On the other hand, many studies have found systematic differences between the physical properties of groups and galaxy clusters (Eckmiller et al. 2011 and references therein).

The purpose of this paper is to statistically compare properties of groups in observations and simulations and to find the most important differences between them. This analysis provides the stepping stone to more detailed studies of individual group properties that can give more strict constraints for the semi-analytical methods (SAM) that incorporate presently all complicated physics related to galaxy formation. Several SAMs have been applied to the Millennium Run to construct galaxies by using the dark matter merger trees in the simulation. Our study is based on the galaxies produced by the semi-analytical procedures by Bertone, De Lucia and Thomas (2007) and Font et al. (2008). Using the mock group catalogue and SDSS groups we study how closely the FOF-groups in simulations resemble the observed galaxy groups. This will tell us how well the distribution of galaxies defined on the basis of SAM represents the real distribution of galaxies in groups. Similar comparison studies between galaxy group catalogues and SAM results have been done, for example, by Weinmann et al. (2006b), Kimm et al. (2009) and Liu et al. (2010).

In Section 2 we present both the observational and mock data sets used in this study and outline the procedure used to construct the group catalogue for the Millennium simulation. We compare the galaxy luminosity functions in observations and simulations, and describe the general statistical properties of the galaxies. In the next section (Section 3) we analyse in detail the statistical properties of galaxy groups in the SDSS galaxy group catalogue and in the mock catalogue. We study the group luminosity functions, group richnesses, rms velocities, virial radii and maximum sizes and cross-correlate them between the mock catalogues and observations. The radial distribution of galaxies in the groups is studied before the conclusions and discussion (Section 4).

## 2 DATA

### 2.1 Observations

As a basis for our analysis we have used groups of galaxies compiled by Tago et al. (2010) for the Sloan Digital Sky Survey seventh data release (SDSS DR7)<sup>1</sup>, (York et al. 2000, Adelman-McCarthy et al. 2008, Abazajian et al. 2009). This group catalogue was derived from the SDSS DR7 main galaxy sample which contains 697920 galaxies. After the extraction process the total number of galaxies used was reduced to 583362, covering the redshift range  $0.009 < z < 0.2$  and about 25 percent of the full sky. A small number of groups ( $\sim 2\%$ ) are located close to the edges of the SDSS field. Since the number of such groups is so small, the possible errors that are caused by this should be also very small and they do not influence the results.

To study the properties of galaxy groups we have selected different volume-limited samples from the DR7 data. By using volume selected samples the comparison with the simulations is free of many selection effects and the calculated distributions can be directly compared. The observed magnitudes of individual galaxies in the SDSS Petrosian  $r$ -magnitude band  $m_r$  are between 12.5 and 17.77. These limits are used for the absolute magnitude limits  $M_r$ . The absolute magnitudes in the group catalogue correspond to the rest frame at the redshift  $z = 0$ . We select four samples S1, S2, S3 and S4 that have faint absolute magnitude limits  $-18$ ,  $-19$ ,  $-20$  and  $-21$ . In this way all galaxies that have  $L_r > L_{\text{lim}}$  are included in the analysis. The  $L_{\text{lim}}$  is simply  $L_{\text{lim}} = 10^{((M_{\odot} - M_r)/2.5)} L_{\odot}$ , where  $M_{\odot} = 4.52$  and  $M_r = m_r - 5 \log(d_{\text{lim}}/10)$ . Thus, the sample luminosity limits are  $L > 0.102 \times 10^{10} h^{-2} L_{\odot}$ ,  $L > 0.256 \times 10^{10} h^{-2} L_{\odot}$ ,  $L > 0.643 \times 10^{10} h^{-2} L_{\odot}$  and  $L > 1.61 \times 10^{10} h^{-2} L_{\odot}$ . In the catalogue by Tago et al. (2010) the group luminosities are also corrected to include the unobserved galaxies, but this correction is not necessary for volume-limited samples, and we have restored the uncorrected values. The group catalogue is compiled using a version of the FOF-algorithm in which the linking length varies with the volume-limited galaxy sample, but it is fixed inside a specific sample. These lengths are 0.250, 0.31, 0.41 and 0.54  $h^{-1}$ Mpc for S1, S2, S3 and S4, correspondingly (see more details in Tago et al. 2010).

The total numbers of groups in the different samples are 5463, 12590, 18973 and 9139 in S1, S2, S3 and S4, correspondingly. Roughly half of the groups are actually galaxy pairs. To scale all the absolute numbers to spatial densities that can be used for comparison, we have calculated the total volumes of the different volume-limited samples. SDSS coverage calculated directly from the data used in this study is 7221 square degrees. Correspondingly, the volumes for different samples are  $1.517 \times 10^6$ ,  $6.541 \times 10^6$ ,  $24.27 \times 10^6$  and  $83.78 \times 10^6 h^{-3} \text{Mpc}^3$  for S1, S2, S3 and S4.

We divide our groups in different classes on the basis of group richness. Galaxy pairs are special groups that have only two members; so we divide the groups into classes with  $N_{\text{gal}} = 2, 3-9$  or at least ten galaxies. The fractions of groups in the volume-limited samples in each class are given in Table 1. We notice that at least 60 percent of all groups are

<sup>1</sup> <http://www.sdss.org/dr7/>

**Table 1.** Fractions of galaxy groups in different richness classes in observations. The numbers of groups  $N_g$  in the Tago et al. (2010) catalogue are given for illustration.

Sample	pairs	$N_{\text{gal}}=3-9$	$N_{\text{gal}} \geq 10$
S1: $M \leq -18$	0.64	0.34	0.021
$N_g$	3498	1965	117
S2: $M \leq -19$	0.65	0.33	0.016
$N_g$	8242	4348	200
S3: $M \leq -20$	0.68	0.31	0.010
$N_g$	12829	6144	196
S4: $M \leq -21$	0.80	0.20	0.00066
$N_g$	7266	1873	6

**Table 2.** Fractions of galaxy groups that have the same richness in the volume-limited and magnitude-limited SDSS group catalogues.

Sample	pairs	$N_{\text{gal}}=3-9$	$N_{\text{gal}} \geq 10$
S1: $M \leq -18$	0.41	0.20	0.0085
S2: $M \leq -19$	0.42	0.21	0.015
S3: $M \leq -20$	0.44	0.22	0.010
S4: $M \leq -21$	0.46	0.29	-

galaxy pairs and the fraction of groups with at least 10 members is only  $<2$  percent. Roughly,  $\sim 30$  percent of groups are intermediate groups with  $N_{\text{gal}}=3-9$  members. The fraction of pairs increases from 0.64 to 0.8 with the luminosity limit of a sample as faint galaxies are dropped. We also give the absolute numbers of groups in different samples in the table.

Tago et al. (2010) compiled also a group catalogue based on the full magnitude-limited galaxy sample. This includes all galaxies that have the Petrosian  $r$ -magnitudes between  $r = 12.5$  and  $r = 17.77$ . The comparison between the volume-limited galaxy groups and magnitude-limited galaxy groups can be used to quantify how the removed galaxies in a certain volume-limited sample affect group definition. For this reason we have calculated the fractions of galaxy groups that have the same number of members in both samples (see Table 2).

More than 40 percent of all galaxy pairs are pairs in both the volume-limited and magnitude-limited samples. For groups with  $N_{\text{gal}}=3-9$  members, 20–30 percent of all groups have the same richness. It is also possible to calculate the fractions of galaxy groups in the magnitude-limited catalogue that are separated into several groups in a volume-limited catalogue. The fractions of multiple groups in a volume-limited catalogue that are single groups in the magnitude-limited catalogue are 0.11, 0.097, 0.071 and 0.025 in the S1, S2, S3 and S4, respectively.

This comparison between the magnitude-limited catalogue and the volume-limited catalogues shows that in reality the group richness and galaxy content are strongly dependent on the magnitude limits. Only a small fraction of groups have exactly the same galaxies in both catalogues. This affects the comparison between the observed and simulated groups, but if the data is calculated in the same way for both groups, the comparison is still reliable.

## 2.2 Simulations

The Millennium Simulation (Springel et al. 2005, hereafter MS) is a cosmological N-body simulation of the  $\Lambda$ CDM model performed by Virgo Consortium, using a customized version of the GADGET2 code. The MS follows the evolution of  $2150^3$  particles from the redshift  $z = 127$  in a box of  $500 h^{-1}\text{Mpc}$  on a side. The cosmological parameters of the MS simulation are:  $\Omega_m = \Omega_{\text{dm}} + \Omega_b = 0.25$ ,  $\Omega_b = 0.045$ ,  $h = 0.73$ ,  $\Omega_\Lambda = 0.75$ ,  $n = 1$ , and  $\sigma_8 = 0.9$ . These values are slightly off from the current best estimate values based on the Planck data:  $h = 0.678$ ,  $\Omega_m = 0.315$ ,  $n = 0.961$  and  $\sigma_8 = 0.829$  (Planck Collaboration XVI 2013). This may have a small effect on the differences that we see in our study, but this effect is very difficult to quantify. We choose the data from the  $z = 0$  snapshot, since the magnitudes in the observational catalogue correspond to the  $z = 0$  magnitudes and possible evolutionary effects are so small that we do not expect that they influence the results.

In our analysis we use two different semi-analytic galaxy formation models: Font et al. (2008) and Bertone et al. (2007) data. These are based on different galaxy formation models (GALFORM (Durham model) and L-Galaxy (Munich model)), respectively. These differ from each other in the halo/subhalo merger tree schemes, as well as in details of the baryonic physics. Several authors (e.g. for GALFORM: Bower et al. 2006, Croton et al. 2006, Font et al. 2008, for L-Galaxy: De Lucia et al. 2006, De Lucia et al. 2007, Guo et al. 2011) have adjusted SAMs for both schemes to reach better agreement with the observational data. These analyses have shown, for example, that the amplitude of the galaxy luminosity function depends strongly on the feedback models. Especially, the bright end of the galaxy luminosity function can be reduced by active galactic nuclei (AGN) feedback models.

Based on the GALFORM scheme, Bower et al. (2006) introduced improved procedure for the feedback from the AGN and the growth of the supermassive black holes. Moreover to improve agreement with satellite galaxy colour distributions with observations, Font et al. (2008) implemented into Bower et al. (2006) version the prescription for ram pressure stripping of the hot gaseous haloes. Similarly, Bertone et al. (2007) developed previous SAM (De Lucia & Blaizot et al. 2007) including the AGN feedback by Croton et al. (2006) and a new procedure for the SN feedback stellar wind model and for the dust attenuation.

The galaxies from the semi-analytical procedure by Bertone, De Lucia and Thomas (2007) are used to construct the main mock catalogue. The Bertone model predicts a lower number of dwarf galaxies than many other models, a feature that fits better with observations. The drawback of their model is that it predicts a larger number of bright galaxies than found in observations. The semi-analytical galaxy catalogue used includes all the necessary information for direct comparison of galaxy group properties. To build a group catalogue for the Bertone SAM galaxies we use the full simulation box that is a cube with the size of  $500 h^{-1}\text{Mpc}$ .

To understand how sensitive our results are for different SAMs, we used the SAM galaxy catalogue by Font et al. (2008). For this sample we also used a cube with the size of  $500 h^{-1}\text{Mpc}$ . The Font data is used as the reference

sample, to show general trends of distributions for qualitative evaluation. The Bertone SAM data is used for the main analysis.

To construct a simulated galaxy group catalogue we start from the general collection of SAM galaxies in the simulation. In the first step, to mimic the observations the galaxies inside the simulation box are transferred to the redshift space. Since the number of groups in observations that are influenced by the edge effects is so small, we don't include the actual SDSS footprint to our analysis. We expect that the error caused by this is so small that it can't be seen in our analysis. In this process a coordinate transformation is applied, where one corner of the cube is taken as the position of the observer (the coordinates 0, 0, 0) and each galaxy is shifted in the line-of-sight direction by its speed vector projection in the line of sight. In this step we include  $30 \text{ km s}^{-1}$  rms error in redshift with Gaussian distribution. However, our tests show that this has only a marginal effect on the distributions and all the conclusions are the same even if this error is ignored. Then the volume limit cuts, as stated earlier, are applied to the data sets, but here we use different abbreviations for the samples: M1, M2, M3 and M4. For the M4 sample a smaller upper cut is applied ( $z$  defined by the distance of  $462 h^{-1} \text{Mpc}$  due to the sample limit), because we want to avoid problems caused by sample asymmetries. After that, we use precisely the same FOF-code, with the same linking lengths as used in Tago et al. (2010). Hence, the method used to construct the SDSS groups and simulated groups is exactly the same and the remaining differences should be due to the spatial distribution of galaxies in the large-scale structure and/or in the properties of galaxies. In Sec. 3.4 we will study, for example, how very close galaxies that would very likely be missed in the SDSS data, may cause some differences. However, since this incompleteness is internal to the published DR7 galaxy catalogue, we cannot model this very accurately.

Using the calculated comoving volumes we normalize the galaxy group property distributions and the spatial densities of simulated data. This allows direct comparison between the volume-limited samples in simulations and observations. The spatial densities of all groups and the numbers of the groups  $N_g$  for different luminosity limits and for group definitions are given in Table 3. The number densities of groups in simulations and observations are similar (within the factor of  $\sim 1.5$ ), but systematically slightly larger for simulated groups in all samples compared with observations. For large groups ( $N_{\text{gal}} \geq 10$ ) the difference is much larger (by a factor of  $\sim 2-6$ ), depending on the sample. The difference is probably due to SAM and the chosen cosmology. Since the number density of galaxies in MS is larger, it is expected that by using the same linking length, there are more groups in the simulated sample than in the SDSS sample. This can be seen by comparing the luminosity functions given in Fig. 1 shown later in the text. Nevertheless, one should keep in mind that it is very difficult to estimate the statistical errors in these values, since the errors include the sample variance that cannot be estimated as we have only one simulation.

In Table 4 we also give the median and mean values for the group masses in the simulation. The masses given in the table include only the mass of the galaxies within the sample magnitude limits; faint galaxies outside the observa-

**Table 3.** Numbers of galaxy groups with  $N_{\text{gal}} \geq 2$  and  $N_{\text{gal}} \geq 10$  for the Bertone SAM galaxies. The data is divided into four different samples. We give also the group number densities for the simulations (Bertone) and for the observations (Tago) in units of  $h^3 \text{Mpc}^{-3}$ .

Sample	$N \geq 2$	$N \geq 10$
M1: $M \leq -18$	4419	209
Bertone $N_\rho$	$4.02 \times 10^{-3}$	$1.90 \times 10^{-4}$
Tago $N_\rho$	$3.47 \times 10^{-3}$	$7.43 \times 10^{-5}$
M2: $M \leq -19$	9989	329
Bertone $N_\rho$	$2.04 \times 10^{-3}$	$6.74 \times 10^{-5}$
Tago $N_\rho$	$1.85 \times 10^{-3}$	$2.94 \times 10^{-5}$
M3: $M \leq -20$	21189	418
Bertone $N_\rho$	$1.12 \times 10^{-3}$	$2.25 \times 10^{-5}$
Tago $N_\rho$	$7.52 \times 10^{-4}$	$7.77 \times 10^{-6}$
M4: $M \leq -21$	15755	97
Bertone $N_\rho$	$2.36 \times 10^{-4}$	$1.45 \times 10^{-6}$
Tago $N_\rho$	$1.05 \times 10^{-4}$	$6.89 \times 10^{-8}$

**Table 4.** Mean and median masses (in units of  $10^{12} h^{-1} M_\odot$ ) of the galaxy groups in the Bertone SAM data.

Sample	Mean	Median
$M \leq -18$ , All	$4.22 \pm 0.3$	1.10
Pairs	$1.15 \pm 0.04$	6.49
3-9	$4.35 \pm 0.2$	2.37
$\geq 10$	$42.2 \pm 5$	22.1
$M \leq -19$ , All	$6.18 \pm 0.2$	1.73
Pairs	$2.04 \pm 0.04$	1.11
3-9	$7.61 \pm 0.2$	4.04
$\geq 10$	$66.8 \pm 5$	37.6
$M \leq -20$ , All	$13.7 \pm 0.3$	4.25
Pairs	$5.93 \pm 0.1$	2.82
3-9	$22.4 \pm 0.6$	10.6
$\geq 10$	$163 \pm 10$	101
$M \leq -21$ , All	$46.7 \pm 1$	23.2
Pairs	$30.1 \pm 0.8$	17.6
3-9	$97.7 \pm 4$	58.9
$\geq 10$	$238 \pm 40$	235

tional window are not included. The group mass is simply the sum of all virial masses of the galaxies in the group. This table describes the typical group or clusters masses in different samples. Groups with  $N_{\text{gal}} \geq 10$  members are an order of magnitude more massive than the mean value for all groups. Groups in M1 have masses  $\sim 4-40 \times 10^{12} h^{-1} M_\odot$  and for the most distant groups in M4 the masses are considerably larger, between  $\sim 0.5-2 \times 10^{14} h^{-1} M_\odot$ .

**Table 5.** Galaxy number densities in units of  $h^3\text{Mpc}^{-3}$  in the Millennium simulation (MS) and SDSS.

Sample	Bertone	Font	SDSS
$M \leq -18$	$3.26 \times 10^{-2}$	$4.00 \times 10^{-2}$	$2.58 \times 10^{-2}$
$M \leq -19$	$1.92 \times 10^{-2}$	$2.12 \times 10^{-2}$	$1.40 \times 10^{-2}$
$M \leq -20$	$8.26 \times 10^{-3}$	$7.78 \times 10^{-3}$	$5.88 \times 10^{-3}$
$M \leq -21$	$1.66 \times 10^{-3}$	$1.88 \times 10^{-3}$	$1.20 \times 10^{-3}$

### 3 COMPARISON BETWEEN GALAXIES IN THE SIMULATION AND THE SDSS GALAXIES

Before we start to compare the group properties of simulations with observations, we analyse the galaxy luminosity functions. We give the galaxy number densities in different volume-limited samples in Table 5.

This Table shows certain differences between simulations and observations. Firstly, all cosmological simulations are realizations of a set of initial conditions and the subsequent large-scale structure is always different. Secondly, all SAMs populate haloes with galaxies in a different way and include different physical processes and approximations in their recipes.

The galaxy luminosity functions for SDSS and for the Bertone et al. (2007) and Font et al. (2008) SAM galaxies applied to the Millennium data, are shown in Fig. 1. For the Bertone data we use dust corrected magnitudes, but for the Font data only  $M_r$  is given. This may introduce a small shift in the luminosity function for the Font data (see, e.g., Tempel et al. (2011)). Both SAMs include AGN feedback. In the same figure we show the luminosity limits used in our volume-limited samples as vertical lines. The agreement between the observations and simulations is relatively good between  $-21.5 < M_r - 5 \log h < -18$ , but for the magnitudes  $M_r - 5 \log h < -21.5$  the Millennium SAM data clearly overestimate the number of luminous galaxies. Font et al. (2008) compared the simulations against the 2dFRS data and they agree rather well, but our study shows that their SAM data do not agree that well with the SDSS data. The most feasible reason for this is in intrinsic differences of the SDSS and 2dFGRS galaxy luminosities, since these galaxy surveys have different sky coverage and wavebands. Differences of the surveys are seen especially at the bright end of the luminosity function.

It seems that this problem is very difficult to eliminate (especially for the  $r$ -band) in the SAM procedure; the same problem remains in a recent study by Guo et al. (2011), albeit not that severe. Although the difference seems to be quite drastic, for our analysis this difference is not that significant, since most galaxies belong to the region where all distributions agree quite well. The most luminous galaxies are typically in rich groups that consist of rare objects, and therefore in the statistical study their effect on the general group properties is rather small.

In the Fig. 1 we also show the luminosity function calculated by Blanton et al. (2003). They derived the best-fit Schechter function using the older version of the SDSS catalogue and obtained the values for the parameters  $\Phi_* = (1.49 \pm 0.15) \times 10^{-2} h^3 \text{Mpc}^{-3}$ ,  $M_* - 5 \log_{10} h = -20.44 \pm 0.01$

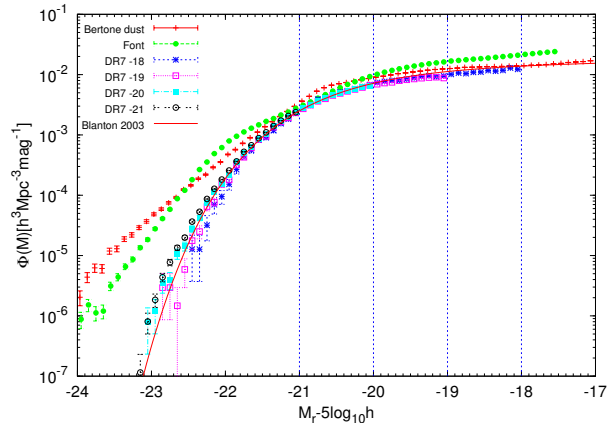


**Figure 1.** The luminosity function for the  $r$ -band of all galaxies in the Bertone SAM based on the Millennium Simulation (MS), compared with the observed SDSS luminosity function as given in Tago et al. (2010), for four different volume-limited samples. The luminosity function derived in Blanton et al. (2003) is given for comparison.

and  $\alpha = -1.05 \pm 0.01$ . This agrees very well with the Tago et al. (2010) galaxy data.

#### 3.1 Group luminosity functions

Here we compare the group luminosity functions that give the number of groups per unit volume as a function of total group luminosity ( $L_{\text{gr}}$ ). The luminosities of all galaxies that belong to the group are summed together to calculate the group luminosity  $L_{\text{gr}} = L_{\text{main}} + \sum L_{\text{satellite}}$ , where  $L_{\text{main}}$  is the luminosity of the main galaxy and  $L_{\text{satellite}}$  is the luminosity of a satellite galaxy in the same group. The main galaxy is always the most massive galaxy in the group obtained from the simulation and in the observations, the main galaxy is the brightest galaxy in a group. The luminosity functions for each volume-limited sample are given in Fig. 2. The lower limit of the group luminosities is determined by the luminosity limit for individual galaxies and therefore the distribution gets more narrow for bright groups. In observations there are systematically less bright groups than in simulations, but the overall agreement is quite good. This difference is mostly because in simulations there are more luminous galaxies. The agreement is very good in the  $M \leq -18$  sample for intermediate groups ( $N_g = 3-9$ ), and the greatest differences are seen for rich groups. The difference is quite drastic in the  $M \leq -21$  sample, for which the whole distribution is shifted towards smaller magnitudes.

The fact that simulations give too many and too bright groups is partly due to too high luminosities of some galaxies (see the galaxy luminosity function). Our more detailed analysis of the Bertone SAM data revealed that there are some galaxies with exceptionally low  $M/L$  ratio. For this reason the bright end of the luminosity function differs considerably from the observations. In the dust-corrected data, the number of these luminous and light galaxies is reduced, but obviously not all of them. About 7–10 percent of Bertone’s dust-corrected galaxies at  $M \leq -22$  seem still to have exceptionally low  $M/L$  ratio at the given mass. Extracting these objects from Bertone’s data gives a luminosity

function which fits better with observations. This modification changes mainly the bright end of the luminosity function, which would not be the result of the variation of the  $\sigma_8$  parameter. This hints that dust correction is too inefficient in SAMs or there are problems modelling the physics of galaxy formation. Guo et al. (2011) compared the SDSS luminosity function with their SAM and they reported, that their model overpredicts the abundance of luminous galaxies likely because of problems in their dust modelling. This does not exclude the effect, which may come from the possible difference of  $\sigma_8$  between theory and observations. For example, Yang et al. (2005) showed that the multiplicity and luminosity functions of groups are inconsistent with the observational data if  $\sigma_8 = 0.9$  is used, but  $\sigma_8 = 0.7$  gives a perfect fit. Also, van den Bosch et al. (2005) showed that simulations with  $\sigma_8 = 0.9$  cosmologies are unable to match the abundances of central and satellite galaxies with observations.

Another reason for the mismatch between simulations and observations is that the richness distribution is different for rich groups (see Fig. 3). In simulations there are more rich groups that increase the number of luminous groups. Especially, the differences are notable for rich groups in the last two volume-limited samples. These samples typically contain only the most luminous galaxies and it is expected that the group luminosity is also overestimated, due to the unrealistically bright massive galaxies. The Font data and the Bertone data MS both give almost identical distributions for all samples. Hence, different SAMs give very similar results although the luminosities of galaxies are modelled in different ways.

To compare our group luminosity functions to other observational studies we use the data from the study by Yang et al. (2007). They constructed the group catalogue based on the DR4 data using an adaptive halo based group finder (Yang et al. 2005b) and calculated the corresponding volume-limited samples and the luminosity functions for the groups  $\Phi(L_{gr})$ . They divided the sample into two different classes: groups with  $M_r - 5 \log h \leq -19.5$  and groups with  $M_r - 5 \log h \leq -18.5$ . Since our magnitude limits differ slightly from theirs and direct comparison is not possible, we show both distributions in our figures. The correspondence is relatively good, although the method for group construction is different. The main difference is at large luminosities. The Tago et al. (2010) group catalogue does not contain as many luminous groups ( $\log L_{gr}[10^{10} L_\odot] \gtrsim 1.8$ ) as the Yang et al. (2009) catalogue. In this respect the simulations agree better with Yang et al. (2009) data than with the Tago et al. (2010) catalogue although simulated groups have been constructed using the same algorithm as in Tago et al. (2010).

### 3.2 Group richness

Multiplicity function estimates provide one of the key constraints on the galaxy group properties. The group richness distributions  $N_{gal} = N_{satellite} + 1$  (the number of galaxies in a group, here  $N_{satellite}$  is the number of satellite galaxies), are shown in Fig. 3. The first bin is for pairs and the distributions extend up to 100 members. There is a clear exponential trend and we fitted straight lines to the distributions to see how the slope values depend on the absolute magnitudes. For the SDSS groups Berlind et al. (2006) found that the

multiplicity functions are well fitted by power-law relations, with the best-fit slopes of  $-2.49 \pm 0.28$ ,  $-2.48 \pm 0.14$  and  $-2.72 \pm 0.16$  for the absolute magnitude limits of  $M_r \leq -18$ ,  $-19$  and  $-20$ . These absolute magnitude limits are approximately the same as for our first three samples. The least-square fit to our observational data gives the values  $-2.02 \pm 0.18$ ,  $-2.12 \pm 0.17$ ,  $-2.26 \pm 0.19$  and  $-3.29 \pm 0.24$  for the  $M_r \leq -18$ ,  $-19$ ,  $-20$  and  $-21$  samples, respectively. To include the Poisson errors we used  $1/\sqrt{N}$  weights during the fit, where  $N$  is the number of groups in a bin. Our values are slightly smaller from those of Berlind et al. (2006), but there is a similar trend that for brighter groups the slope is steeper. Without using weights in the fit, the slope values are closer to the ones obtained by Berlind et al. (2006). Since our samples in simulations consist of groups with different mean masses (see Table 4), we can conclude that richness distribution is a function of group mass. For massive groups the distribution is steeper than for the less massive groups. Analogously, the same should apply for observational data.

For small groups (the first three bins) the agreement between all groups is very good. As the number of members in the groups starts to exceed 10, the distributions start to deviate. The MS group richness distribution, that should be the same in the ideal case, is above the SDSS distribution. As for luminosity distributions, the Font data and Bertone data give results that are very close to each other. Thus, we see that in the Millennium SAM data there are too many rich and luminous groups compared with observations and the differences are larger for richer groups.

The richness distribution can also be calculated for the Yang et al. (2007) group catalogue. We used their sample III that contains 300049 groups extracted from the SDSS DR4 galaxy data. Their catalogue of galaxy groups is not volume-limited, but it is still interesting to compare the richness distribution. They used the magnitude limit  $M_r - 5 \log h \leq -19.5$  that is between these for our two first samples. The richness distribution is shown in the first panel (crosses) with an arbitrary scaling, since the total volume of their catalogue is not known. The agreement between our SDSS richness function and theirs is very good.

It is also interesting to compare our results with those for the more recent GAMA galaxy group catalogue (Robotham et al. 2011). Their group catalogue is not volume-limited either, but the comparison is still valuable. Their richness distribution also follows a linear trend, especially for their mock catalogue, with the estimated slope value of  $\sim -1.7$ . It is expected that the distribution is not as steep as in the volume-limited catalogue, since in their magnitude-limited sample there are more faint galaxies and group richnesses are typically higher. They noticed that the number of high-richness systems is significantly different between the observational data and the mocks, but for low-richness systems the distributions agree better. This is exactly the same feature that we see in our data. Their interpretation is that SAM (Bower et al. 2006, GALFORM) populates more massive haloes with an excessive number of faint satellite galaxies, a feature that is reported to be a problem in this model (Kim et al. 2009).

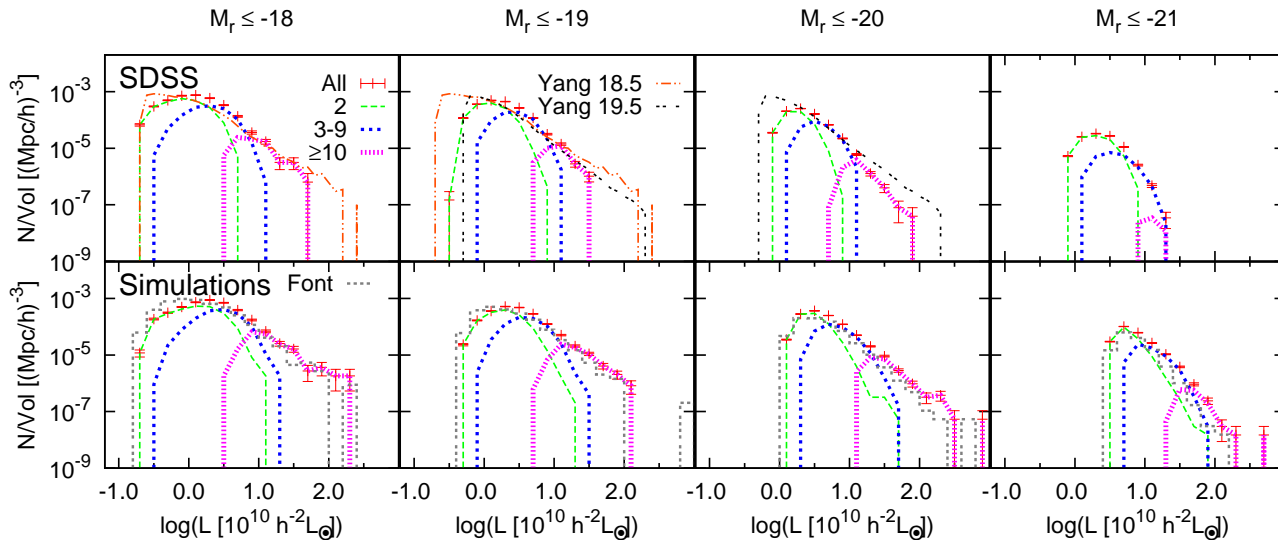


**Figure 2.**  $R$ -band luminosity functions for groups in the SDSS data (upper row) and for the group catalogue obtained from the Bertone SAM based on MS (lower row), for four different volume-limited samples. All groups with two or more member galaxies are included. In all panels we show the total distribution as red points and the Poisson errors in the bins by red bars. The distributions for galaxy pairs (green dashed line), for groups with  $N_{\text{gal}}=3-9$  members (blue dotted line) and for groups with  $N_{\text{gal}}\geq 10$  members (magenta dash dotted line) are also given. The luminosity functions for the DR4 groups by Yang et al. (2009) are shown as two dashed lines for two different samples.

### 3.3 Projected virial radii estimator

One of the basic parameters of a galaxy group is its virial radius. To estimate the projected virial radius we use the harmonic mean of the projected separations:

$$R_{\text{vir}} = \left( \frac{1}{n_{\text{pairs}}} \sum \frac{1}{r_{ij}} \right)^{-1}, \quad (1)$$

where  $r_{ij}$  is the mutual projected angular diameter distance between galaxies  $i$  and  $j$  for  $n_{\text{pairs}}$  pairs. If the number of galaxies in a group is  $n$ , then  $n_{\text{pairs}} = n(n-1)/2$ . For large groups this estimator becomes tightly correlated with the real virial radius, but this equation is not good for small groups. However, it is used here, since in the SDSS comparison paper it was calculated in this way and we call it simply as virial radius. We will use the virial radius estimator as a scaling factor in the analysis of radial distance distribution of galaxies in a later section. In the simulation we know also the virial radius of the main galaxy, but this and the virial radius of the group are only weakly correlated. The distributions of projected virial radii for all groups are shown in Fig. 4.

In Table 6 we show the mean values of the virial radii for simulations and observations. For these estimates we have ignored galaxy pairs, since these bias the results towards small values. For the observations, the mean values vary between 0.14 and 0.36  $h^{-1}$ Mpc and a general trend is that  $\langle R_{\text{vir}} \rangle$  is larger for those groups that do not include faint galaxies ( $M \leq -21$ ) compared with the groups that include also faint galaxies ( $M \leq -18$ ). Rich groups are also typically larger in size than loose groups and therefore  $\langle R_{\text{vir}} \rangle$  is systematically larger for rich groups. The sample  $M \leq -21$  extends much further in distance than the  $M \leq -18$  sample and the linking length in the FOF-algorithm increases with the absolute magnitude limit. Therefore there are much

**Table 6.** Mean values of the virial radii for all  $N_{\text{gal}}=3-9$  and  $N_{\text{gal}}\geq 10$  distributions shown in Fig. 4, in  $h^{-1}$ Mpc units.

Sample, $N_{\text{gal}}$	Simulations (Mean)	SDSS (Mean)
$M \leq -18$ , 3-9	0.122±0.002	0.136±0.001
$\geq 10$	0.165±0.005	0.200±0.005
$M \leq -19$ , 3-9	0.123±0.001	0.165±0.001
$\geq 10$	0.164±0.003	0.242±0.004
$M \leq -20$ , 3-9	0.128±0.0008	0.216±0.001
$\geq 10$	0.166±0.003	0.307±0.006
$M \leq -21$ , 3-9	0.120±0.001	0.274±0.003
$\geq 10$	0.156±0.007	0.355±0.03

fewer faint galaxies (less massive) in the  $M \leq -21$  sample than in the  $M \leq -18$  sample and at large distances there are fewer small groups that have only a few members, if all galaxies could be observed. In the simulations  $\langle R_{\text{vir}} \rangle$  does not behave in the same way – it is close to 0.12–0.16  $h^{-1}$ Mpc for all the samples.

For all distributions, there are clear differences between the simulations and the SDSS data (Fig. 4). Firstly, in the simulations there are many more small groups with  $\log R_{\text{vir}} < -1.5$  than in observations. The agreement is the best near the mode, but before and after the differences are large. For loose and rich groups the distributions are shifted towards larger  $R_{\text{vir}}$ -values as we move from the  $M \leq -18$  sample to the  $M \leq -21$  sample. Numerically the effect of galaxy pairs on the distributions is remarkable. The distributions are suddenly cut at a certain distance due to the linking length value in the FOF-algorithm. The observational limitations that explain the discrepancy between the

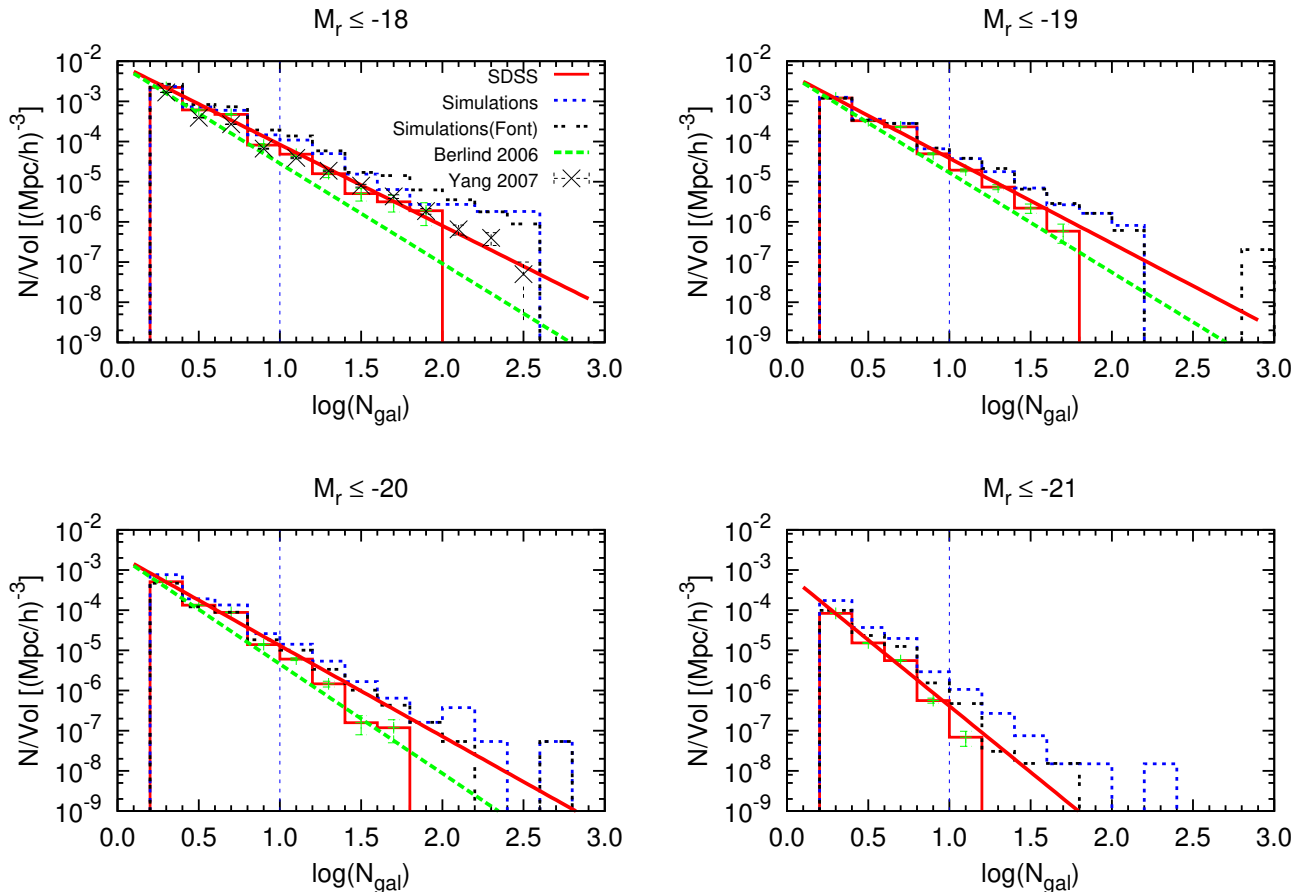


**Figure 3.** Comparison of the group richness (number of galaxies in a group) in the SDSS (solid red line histogram) and in the Bertone SAM based on MS. The Font data is given for comparison as well as the slopes given in Berlind et al. (2006) for the first three samples. Best-fitted slopes for the SDSS data are shown as red solid lines. In the first panel the richness distribution by Yang et al. (2007) is also shown.

SDSS and the mock data at small  $R_{\text{vir}}$ -values will be described in more detail in the next section where we study the maximum projected size distributions. Fig. 4 shows that if galaxy pairs are removed from the analysis, the agreement between different samples is much better and the shapes of the distributions are closer to each other. However, the same observational bias affects also loose and rich groups, but not that significantly. The Font data and the Bertone data give both rather similar distributions.

### 3.4 Group sizes

Another parameter that can be used to characterize a group is the maximum projected galaxy pair separation  $R_{\text{max}}$  in the group. We take that as the definition of the group size. The group size distributions are very similar to the  $R_{\text{vir}}$  distributions (Fig. 5), but the disagreement between the simulations and observations is more obvious for  $\log(R_{\text{max}}/h^{-1}\text{Mpc}) < -1$ . The largest differences are again for small groups. For the first two samples, the simulations have rather similar distributions to the SDSS distributions for large groups, excluding galaxy pairs. The group size distributions have mode values at  $\sim 0.3 h^{-1}\text{Mpc}$ , that is mostly

**Table 7.** Mean values of group sizes for all  $N_{\text{gal}} = 3-9$  and  $N_{\text{gal}} \geq 10$  distributions shown in Fig. 5 (in  $h^{-1}\text{Mpc}$  units).

Sample, $N_{\text{gal}}$	Simulations (Mean)	SDSS (Mean)
$M \leq -18, 3-9$	$0.290 \pm 0.005$	$0.286 \pm 0.003$
$\geq 10$	$1.11 \pm 0.2$	$0.788 \pm 0.03$
$M \leq -19, 3-9$	$0.293 \pm 0.002$	$0.354 \pm 0.003$
$\geq 10$	$0.842 \pm 0.02$	$0.948 \pm 0.02$
$M \leq -20, 3-9$	$0.306 \pm 0.002$	$0.467 \pm 0.003$
$\geq 10$	$0.954 \pm 0.04$	$1.19 \pm 0.03$
$M \leq -21, 3-9$	$0.299 \pm 0.005$	$0.576 \pm 0.006$
$\geq 10$	$1.18 \pm 0.15$	$1.50 \pm 0.2$

due to the galaxy pairs that peak at this distance. The peak is artificially sharp due to the chosen linking lengths that vary between  $0.25-0.54 h^{-1}\text{Mpc}$ ; the peaks are located close to the linking lengths. We give in Table 7 the mean values of the group sizes.

As for the  $R_{\text{vir}}$ -distributions, for rich groups ( $N_{\text{gal}} \geq 10$ ) the agreement between mock groups and observations is rel-



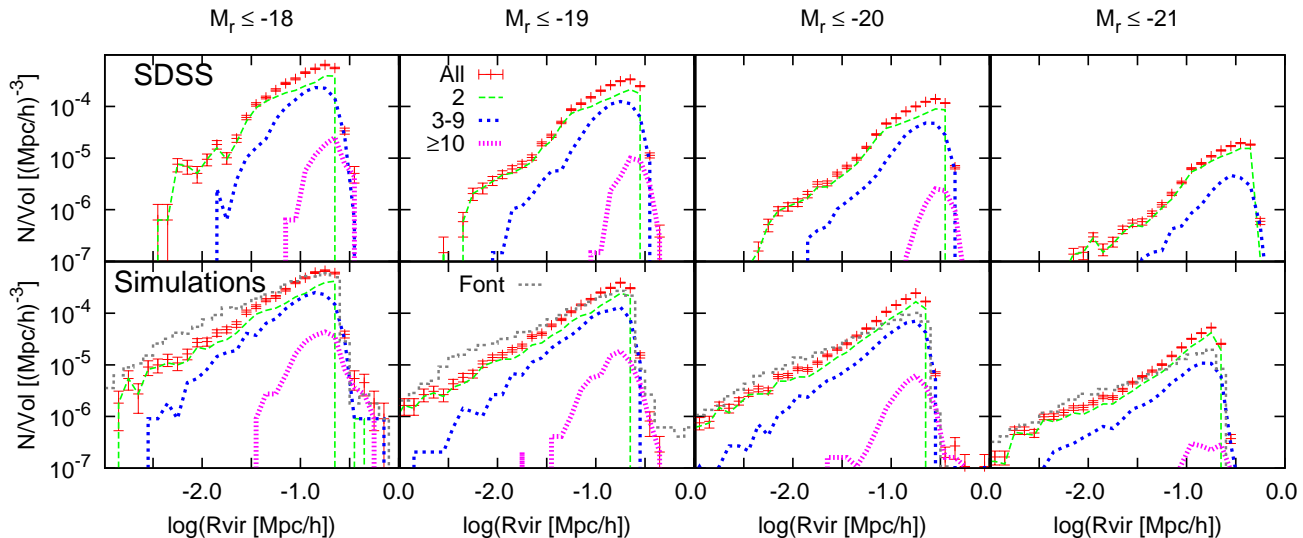


**Figure 4.** Comparison of the distributions of virial radii for SDSS and for Bertone SAM based on MS. The total distribution is shown as red points with the Poisson errors in the bins. The distributions for galaxy pairs (green dashed line), groups with  $N_{\text{gal}}=3-9$  members (blue dotted line) and groups with  $N_{\text{gal}}\geq 10$  members (magenta dotted line) are also given.

atively good. In observations the mean group sizes are systematically larger for the  $M \leq -21$  than for the  $M \leq -18$  sample.  $\langle R_{\text{max}} \rangle$  varies from  $0.29h^{-1}\text{Mpc}$  to  $0.58h^{-1}\text{Mpc}$  for loose groups and from  $0.8h^{-1}\text{Mpc}$  to  $1.5h^{-1}\text{Mpc}$  for rich groups. These values are  $\sim 2$  times larger than for the virial radii. In simulations the mean group sizes behave differently and they remain rather constant ( $0.3h^{-1}\text{Mpc}$ ) for the groups with  $N_{\text{gal}}=3-9$  for all samples. Only for the  $M \leq -18$  sample do the values agree quite well between simulations and observations. For groups with  $N_{\text{gal}}\geq 10$  the mean sizes are larger for the  $M \leq -21$  sample than for the  $M \leq -18$  sample, but still those are smaller than for the SDSS data, excluding the  $M \leq -18$  sample. Also for the  $R_{\text{max}}$ -distribution, the Font data produces similar results to the Bertone data, although some differences can be seen.

The smallest groups, galaxy pairs, have been extensively studied by Patton et al. (2011) for the SDSS DR7 (for DR4 see also Ellison et al. (2010) and Ellison et al. (2008)). They found that the fraction of red galaxies in pairs is higher than that of a control sample and the difference is likely due to the fact that galaxy pairs reside in higher density environments than non-paired galaxies. They also noted an important selection effect that needs to be taken into account. Fibre collisions in the original SDSS data cause small-scale spectroscopic incompleteness at small galaxy separations (Strauss et al. 2002). In Ellison et al. (2008) it is estimated that 67.5 percent of pairs at angular separations below  $55''$  have been missed due to this effect, even when the influence of overlap between adjacent plates and the use of two or more plates in some regions is considered. Taking into account the adopted cosmology and the  $55''$  criterion we have estimated the group size thresholds after which the incompleteness in the distributions at a given distance starts (the smaller the size, the larger the incompleteness). These limits for  $\log(R_{\text{max}}[h^{-1}\text{Mpc}])$  are  $-1.46$ ,  $-1.28$ ,  $-1.11$  and  $-0.955$  for different samples. In Fig. 5 the limits are shown as vertical dashed lines in the top panels. Due to this selection effect, the group size distributions for the SDSS start

to deviate from the mock catalogue distributions near these limits. It is expected that the same limitations affect also richer groups and, in fact, this is also seen in Fig. 5. The fraction of small groups with  $N_{\text{gal}}=3-9$  members in the SDSS is smaller than in simulations. For  $N_{\text{gal}}\geq 10$  groups this effect is not that significant any more, since the group sizes are typically very large. The observed distributions are not as smooth as for the simulations. The minimum size of the SDSS groups  $\sim 10 h^{-1}\text{kpc}$  is also due to the same limitation.

To qualitatively test how close pair incompleteness could maximally influence the results we removed randomly one of the galaxies, from all galaxies that are within  $55''$  (in projected separation) from each other in the mock data. By removing all close galaxies, we removed a number of close pairs, but richer groups were also affected by this procedure (Fig. 6). The size distributions agree then much better with observations, especially for the  $M \leq -18$  and  $M \leq -19$  samples. The distributions for larger groups agree also better, but the difference is not as large as for pairs. In the last two samples ( $M \leq -20$  and  $M \leq -21$ ) there are significant differences as before, but the pair removal behaves as expected. It is not surprising that this correction procedure does not give a perfect match, since the  $55''$  rule is not absolute, and it is very difficult to model the incompleteness effect precisely.

Some of the differences in the distributions at small scales may also be due to the SAM and the used cosmology. In the Bertone et al. (2007) model, subhalo orbits were followed under the influence of the tidal truncation and stripping until the resolution limit of the simulation was reached. Due to the limited resolution of the simulations, part of those subhaloes for which DM haloes are considerably disrupted, lose their DM halo, but retain their galaxy properties formed earlier in the subhalo. Once the resolution limit is reached, these "orphan" galaxies are placed on most bound DM particles of the former DM haloes. Subsequently, merger time (due to dynamical friction) of the orphan galaxy with the

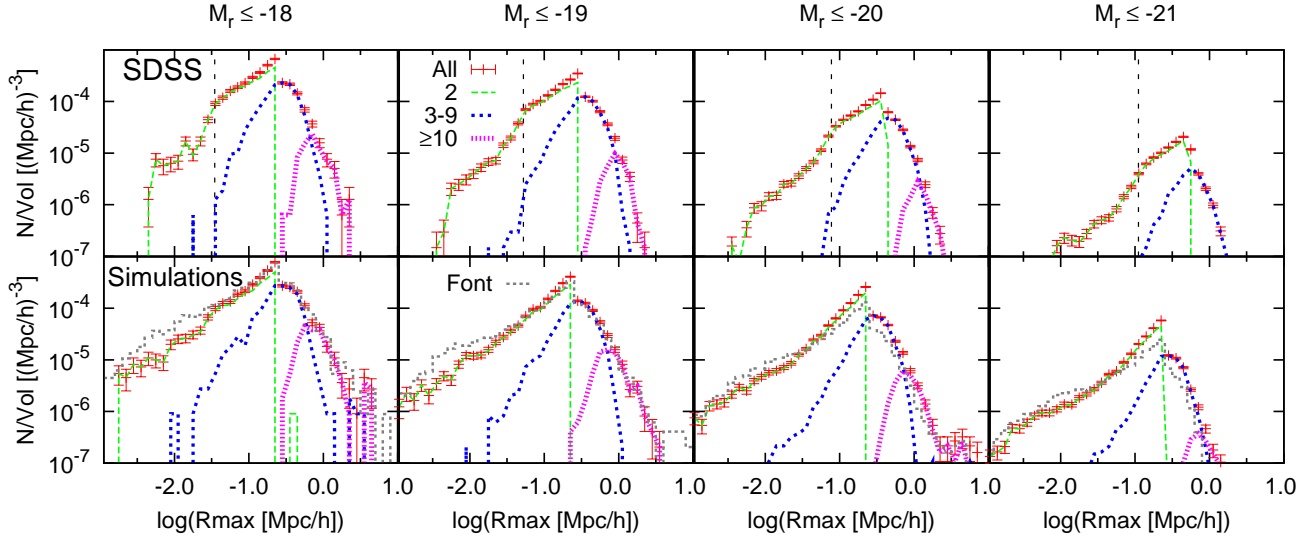


**Figure 5.** Comparison of the group size distributions for SDSS and for Bertone SAM based on MS. The total distribution is shown as red points together with the Poisson errors in the bins. The distributions for galaxy pairs (green dashed line), groups with  $N_{\text{gal}} = 3-9$  members (blue dotted line) and groups with  $N_{\text{gal}} \geq 10$  members (magenta dotted line) are also given. Black dashed vertical lines in the SDSS panels show the incompleteness limits calculated using the  $55''$  criterion described in chapter 3.4.

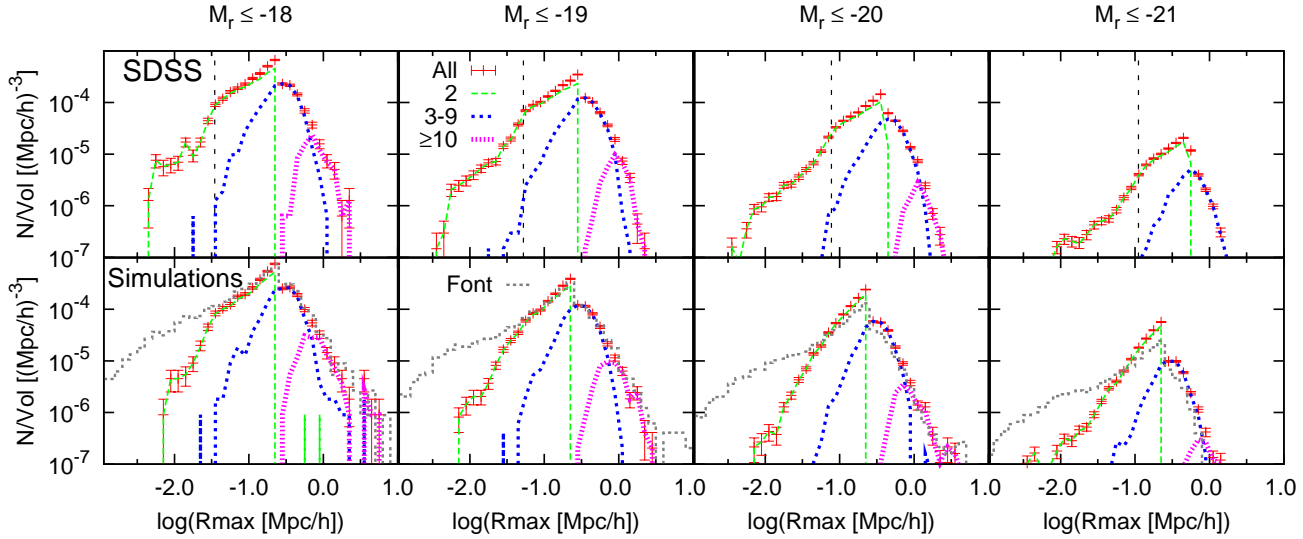


**Figure 6.** Comparison of the group size distributions for the SDSS and for the modified mock data. All neighbour galaxies that lie closer than  $< 55''$  are randomly removed from the simulated data. Otherwise the figure is the same as Fig. 5.

central galaxy is estimated using the analytical formula of Binney & Tremaine (1987). In Bertone et al. (2007), SAM orphan galaxies are not disturbed during the dynamical friction time. This assumption may overestimate orphan galaxy luminosities (Bryan et al. 2008). However, the orphans are not those galaxies that have exceptionally low  $M/L$  ratio mentioned in chapter 3.1. Font et al. (2008) did not follow full orbital evolution of subhaloes and in their model subhaloes are merged according to the dynamical friction time formula. Thus, the Font et al. (2008) model does not include orphans. In the Bertone et al. (2007) simulations orphans are denoted as "type2" haloes and we have included these in our analysis.

Weinmann et al. (2010) tested how the resolution limit

affects the capability of MS (using the De Lucia & Blaizot et al. (2007) model) to follow subhalo evolution. They concluded that MS can be used to follow subhalo evolution to high accuracy for infalling subhaloes with DM mass larger than  $10^{11} M_{\odot} h^{-1}$ .

Guo et al. (2011) calculated the two-point correlation function and analysed galaxy clustering for MS and for the Millennium II (Boylan-Kolchin et al. 2009) simulations at small scales and found out that for stellar masses  $9.77 < \log M_* < 10.77$  and for scales  $< 1 h^{-1} \text{Mpc}$ , galaxies are more clustered in simulations than in observations (SDSS DR7). Orphan galaxies account for almost half of all cluster members with  $M_* > 10^{10} M_{\odot} h^{-1}$  and thus galaxy abundance in clusters is underpredicted in MS. They note

**Table 8.** Mean values of  $\sigma_v$  of galaxy groups for all  $N_{\text{gal}}=3-9$  and  $N_{\text{gal}}\geq 10$  group distributions shown in Fig. 7 (in units of  $\text{km s}^{-1}$ ).

Sample, $N_{\text{gal}}$	Simulations (Mean)	SDSS (Mean)
$M \leq -18, 3-9$	$97.5 \pm 1$	$98.7 \pm 1$
$\geq 10$	$202 \pm 6$	$229 \pm 9$
$M \leq -19, 3-9$	$113 \pm 1$	$119 \pm 0.9$
$\geq 10$	$238 \pm 5$	$258 \pm 7$
$M \leq -20, 3-9$	$144 \pm 1$	$149 \pm 1$
$\geq 10$	$284 \pm 6$	$320 \pm 8$
$M \leq -21, 3-9$	$183 \pm 2$	$195 \pm 2$
$\geq 10$	$371 \pm 19$	$360 \pm 30$

that the reason may be that galaxy disruption is not modelled properly in SAM or then the slightly wrong  $\sigma_8$ -value in MS that follows DM halo and subhalo evolution may cause this difference. In Bertone’s data (used in this paper), about 18 percent of the  $M \leq -18$  galaxies are classified orphans (type 2).

### 3.5 Group rms velocities

To compare dynamical properties of groups, we calculated the rms velocities for groups:

$$\sigma_v = \left( \frac{\sum_{i=1}^N |\vec{v}_i - \vec{v}_{\text{mean}}|^2}{n-1} \right)^{1/2}, \quad (2)$$

where  $\vec{v}_i$  is the velocity of the member galaxy  $i$ ,  $n$  is the number of galaxies in the group and  $\vec{v}_{\text{mean}}$  is the mean velocity of galaxies. We use this estimator for the group velocity differences because it is also used in the Tago et al. (2010) catalogue. For pairs and small groups  $\sigma_v$  has no real physical meaning, but it can still be calculated to have a complete sample for all groups. The distributions of  $\sigma_v$  are shown in Fig. 7. There is an abundance of groups with the rms velocity close to  $100 \text{ km s}^{-1}$  in all cases, and all the distributions agree very well up to this point. For the  $N_{\text{gal}}=3-9$  and  $N_{\text{gal}}\geq 10$  groups the distributions obtained for observations and simulations differ for the two brightest samples. This is expected since the richness distributions are also different for these cases, but the shapes of the  $\sigma_v$  distributions are similar for all groups and samples. If we compare the mean values of the  $\sigma_v$  distributions (Table 9) we notice that the mean values for the mock groups and the SDSS groups are almost the same within the error bars. For the  $N_{\text{gal}}=3-9$  groups the mean value increases from  $\sim 100 \text{ km s}^{-1}$  to  $\sim 200 \text{ km s}^{-1}$  as we move from the  $M \leq -18$  sample to the  $M \leq -21$  sample. For the  $N_{\text{gal}}\geq 10$  groups the mean value increases from  $\sim 200 \text{ km s}^{-1}$  to  $\sim 400 \text{ km s}^{-1}$ , accordingly.

### 3.6 Correlations between different galaxy group properties

We have studied above the overall distributions of different group properties. To understand the mutual dependencies of group properties we have calculated the linear Pearson

**Table 9.** Correlation coefficients for correlations between  $R_{\text{vir}}$  and  $R_{\text{max}}$ . Galaxy groups with  $N_{\text{gal}}=3-9$  and  $N_{\text{gal}}\geq 10$  group members are included in the analysis. Errors given in the table for the mean values are  $1\sigma^{-1}$  standard deviations of the mean value distributions obtained with the jackknifing test.

Sample, $N_{\text{gal}}$	Simulations	SDSS
$M \leq -18, 3-9$	$0.664 \pm 0.013$	$0.749 \pm 0.010$
$\geq 10$	$0.664 \pm 0.010$	$0.818 \pm 0.012$
$M \leq -19, 3-9$	$0.629 \pm 0.013$	$0.729 \pm 0.008$
$\geq 10$	$0.644 \pm 0.012$	$0.718 \pm 0.014$
$M \leq -20, 3-9$	$0.657 \pm 0.011$	$0.736 \pm 0.007$
$\geq 10$	$0.823 \pm 0.007$	$0.680 \pm 0.016$
$M \leq -21, 3-9$	$0.630 \pm 0.013$	$0.744 \pm 0.017$
$\geq 10$	$0.504 \pm 0.021$	-

product-moment correlation coefficients  $r$  between the main group properties: group luminosity,  $R_{\text{vir}}$ ,  $R_{\text{max}}$  and  $\sigma$ . The correlations are calculated separately for the observations and for the mock catalogues, as well as separately for the two group populations with  $N_{\text{gal}}=3-9$  members or with  $N_{\text{gal}}\geq 10$ . Galaxy pairs are ignored, since some of the properties are not properly defined for them. In all samples when the correlation coefficient is  $r > 0.15$ , it is significantly different from zero (with  $p < 0.05$ ), since the degrees of freedom ( $N-2$ ) are always large for all  $r$ -values referred to in the text (see Table 1 for the SDSS data). To estimate the precision of sample statistics we use the so called jackknifing method. From the full data sets we derive 100 subsets of available data and calculate correlation coefficients for each subsets. The subsets are selected so that, for the  $N_{\text{gal}}=3-9$  groups we start initially from the groups with  $N=4-10$  members and remove randomly one member from each group. Similarly for  $N_{\text{gal}}\geq 10$  groups we start from the groups with  $N\geq 11$  members. Then all group properties ( $L_g$ ,  $R_{\text{vir}}$ ,  $R_{\text{max}}$  and  $\sigma$ ) are calculated again 100 times. This gives us the distribution of correlation coefficient values. In the following results we give the mean value and the standard deviation of the correlation coefficient distribution. This analysis shows that our results are not very sensitive for resampling, which indicates that groups are mainly real dynamical systems.

In general, calculations show that correlations are usually very similar for different volume-limited samples, but for those parameters that are clearly correlated, we give a complete sample. As expected, the group virial radius  $R_{\text{vir}}$  and the group size  $R_{\text{max}}$  are always very well correlated (Table 9) with  $r=0.50-0.82$  for Bertone SAM data and  $r=0.68-0.82$  for SDSS data. The correlations are systematically larger for the observed groups than for the mock sample. There is no clear difference between  $N_{\text{gal}}=3-9$  groups and  $N_{\text{gal}}\geq 10$  groups. For groups in general,  $R_{\text{vir}}$  is the lower limit of  $R_{\text{max}}$  and typically  $R_{\text{max}} \sim 1.5-2R_{\text{vir}}$  for the  $N_{\text{gal}}=3-9$  groups and  $R_{\text{max}} \sim 2-4R_{\text{vir}}$  for the  $N_{\text{gal}}\geq 10$  groups.

On the other hand, there is no correlation between  $R_{\text{vir}}$  and  $\sigma$  for all groups. The correlation is larger, but still weak between  $R_{\text{max}}$  and  $\sigma$ :  $r=0.1-0.2$  and  $r=0.1-0.7$ , for  $N_{\text{gal}}=3-9$  and  $N_{\text{gal}}\geq 10$ , respectively. The scatter between different samples is large, but there is no systematical differ-

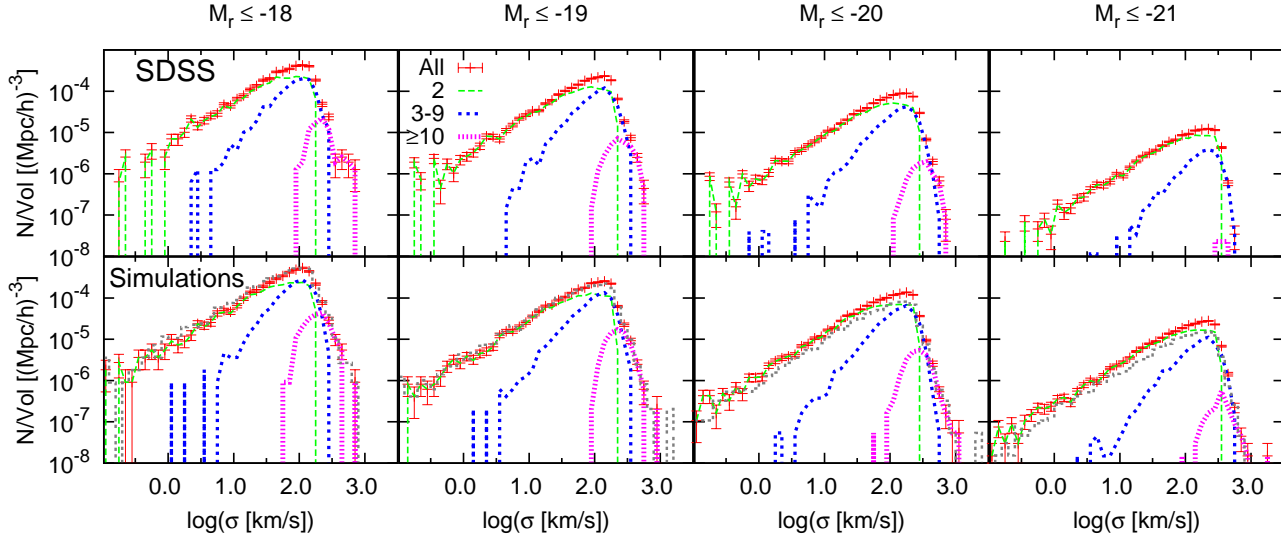


**Figure 7.** Comparison of rms velocity distributions for SDSS and for Bertone SAM based on MS. The total distribution is shown as red points and the Poisson errors are shown in the bins. The modified distributions for galaxy pairs (green dashed line), groups with  $N_{\text{gal}}=3-9$  members (blue dotted line) and groups with  $N_{\text{gal}} \geq 10$  members (magenta dotted line) are also given.

**Table 10.** Correlation coefficients for correlations between  $L_g$  and  $R_{\text{max}}$ . Galaxy groups with  $N_{\text{gal}}=3-9$  and  $N_{\text{gal}} \geq 10$  group members are included in the analysis. Errors given in the table for the mean values are  $1\sigma$  standard deviations of the mean value distributions obtained with the jackknifing test.

Sample, $N_{\text{gal}}$	Simulations	SDSS
$M \leq -18, 3-9$	$0.212 \pm 0.016$	$0.348 \pm 0.015$
$\geq 10$	$0.878 \pm 0.0038$	$0.756 \pm 0.010$
$M \leq -19, 3-9$	$0.234 \pm 0.018$	$0.405 \pm 0.011$
$\geq 10$	$0.703 \pm 0.0080$	$0.572 \pm 0.013$
$M \leq -20, 3-9$	$0.337 \pm 0.010$	$0.443 \pm 0.0085$
$\geq 10$	$0.783 \pm 0.0036$	$0.461 \pm 0.014$
$M \leq -21, 3-9$	$0.271 \pm 0.015$	$0.505 \pm 0.016$
$\geq 10$	$0.805 \pm 0.011$	-

**Table 11.** Correlation coefficients for correlations between  $L_g$  and  $\sigma$ . Galaxy groups with  $N_{\text{gal}}=3-9$  and  $N_{\text{gal}} \geq 10$  group members are included in the analysis. Errors for the mean values are  $1\sigma$  standard deviations and those are obtained with the jackknifing test.

Sample, $N_{\text{gal}}$	Simulations	SDSS
$M \leq -18, 3-9$	$0.186 \pm 0.019$	$0.235 \pm 0.016$
$\geq 10$	$0.596 \pm 0.0065$	$0.749 \pm 0.0084$
$M \leq -19, 3-9$	$0.196 \pm 0.018$	$0.296 \pm 0.010$
$\geq 10$	$0.376 \pm 0.012$	$0.486 \pm 0.012$
$M \leq -20, 3-9$	$0.190 \pm 0.010$	$0.320 \pm 0.0086$
$\geq 10$	$0.658 \pm 0.0050$	$0.473 \pm 0.011$
$M \leq -21, 3-9$	$-0.0553 \pm 0.019$	$0.229 \pm 0.018$
$\geq 10$	$0.968 \pm 0.012$	-

ence between the mock data and observations. The dynamical state of the group and the group mass describe very diverse galaxy environments and therefore the correlation between the group size indicators and the velocity distribution is rather weak.

Lastly, we studied the correlations between the group luminosity, that is related to the group mass, and  $R_{\text{max}}$  and  $\sigma$  (Tables 10 and 11). For intermediate groups ( $N_{\text{gal}}=3-9$ ) the correlation is weak:  $r=0.21-0.50$  between  $L_g-R_{\text{max}}$  and  $r=0.0-0.32$  between  $L_g-\sigma$ . For SDSS data the correlations are systematically stronger. For  $N_{\text{gal}} \geq 10$  groups there is substantial correlation  $r=0.46-0.88$  for  $L_g-R_{\text{max}}$ , but for the mock data the correlation is larger than for SDSS data. For correlations between  $L_g-\sigma$   $r=0.38-0.97$ , but the variations are so large that there are no systematic differences. We notice that weak correlation between luminosity and rms velocity for  $N_{\text{gal}}=3-9$  groups may indicate that these groups are not usually virialized. For rich groups larger correlation coefficients supports higher degree of virialization. For example, by comparing simulations and nearby groups of galaxies Niemi et al. (2007) concluded that approximately 20 percent of nearby groups of galaxies are not bound systems. The strong correlation between  $R_{\text{vir}}$  and  $R_{\text{max}}$  makes their distributions quite similar (Figs. 4 and 5). Since the correlations are stronger for rich groups, these distributions are also more similar than for other group populations.

### 3.7 Radial distribution of galaxies in galaxy groups

It is known that in galaxy clusters the observed galaxy distribution follows very well the underlying DM distribution (Carlberg et al. 1997, Biviano & Girardi 2003, van der Marel et al. 2000, Lin, Mohr & Stanford 2004). Many studies have shown that also satellite galaxies roughly follow a NFW profile inside dark matter haloes, although in some studies satellites are less centrally concentrated than the DM (e.g. Yang et al. 2005, Chen 2008, More et al. 2009). However, in groups

and in the systems that do not have a common DM halo, the observed galaxies in groups may have a different radial distribution. We can analyse this by calculating radial number density distributions of galaxies in groups for the SDSS data and for MS.

The observed radial velocities include position errors due to the peculiar velocities of the galaxies in the group. These errors, finger-of-gods, do not influence any other distribution than the radial line-of-sight distributions of galaxies calculated from the group centre. We correct this effect by following the procedure given in Liivamägi, Tempel and Saar (2012). For every galaxy in the group there is the initial distance  $d_{\text{init}}$  that includes the redshift distortion. We give the new distance  $d_{\text{new}}$  to the galaxy by using  $\sigma_v$  and the rms projected distance  $\sigma_d$ . The mean distance of the group members  $d_{\text{gr}}$  is also needed. Then the new distance is calculated as:

$$d_{\text{new}} = d_{\text{gr}} + (d_{\text{init}} - d_{\text{gr}}) \frac{\sigma_d}{\sigma_v/H},$$

where  $H$  is the Hubble constant. It should be noted that this correction is only statistical and  $d_{\text{new}}$  is not always the true 3D distance. However, for the comparison study this is an important correction that needs to be taken into account. By using  $d_{\text{new}}$  and the sky coordinates we then calculate new position vectors  $\mathbf{r}_i$  for the group galaxies.

It is not evident what is the “true” centre of the galaxy group in the observational data. In our calculations the centre of the group refers to the luminosity centre of the group member galaxies. This is calculated in the same way as the centre-of-mass, but instead of masses we use the luminosities of the galaxies. The centre of the group is then

$$\mathbf{R} = \frac{\sum_{i=1}^N L_i \mathbf{r}_i}{\sum_{i=1}^N L_i},$$

where  $\mathbf{R}$  is the position vector of the group centre,  $L_i$  is the luminosity of a galaxy and  $\mathbf{r}_i$  is its position vector. The group-centric distance  $\Delta = |\mathbf{R} - \mathbf{r}_i|$  between the galaxy and the group centre can be then found. Usually the location of the main galaxy (most luminous) position is slightly shifted from the group luminosity centre. For example, in Skibba et al. (2011) they noticed that the fraction of massive groups in which the brightest galaxy is not the central galaxy is very high  $\sim 40\%$ . Similar results have also been reported in Coziol et al. (2009) and Einasto et al. (2012).

To study the spatial distribution of galaxies in groups we calculated the 3D galaxy number density distributions for all groups with  $N_{\text{gal}} \geq 3$ , showing the number of galaxies at a certain normalised distance  $\Delta/R_{\text{vir}}$  from the group luminosity centre (Fig. 8). The results are given only for the  $M \leq -18$  samples, because the distributions are similar in other samples and this sample includes the richest groups (see Fig. 3). For comparison also the distributions for very rich groups ( $N_{\text{gal}} \geq 20$ ) are given (only 5 in the SDSS sample). In addition to the normal mock catalogue, we also show the distributions for the modified mock catalogue from which all close pairs are removed in the same way as in Sec. 3.4. Fig. 8 shows that after this correction (blue squares in the figure) the observed and theoretical distributions are closer to each other. Without the correction, the observed galaxy distribution significantly differs from the galaxy distributions in the simulation. The left panels show

the radial distributions up to  $\Delta \sim 30R_{\text{vir}}$  in the logarithmic scale and the right panels show only the inner parts of groups (up to the virial radius) in the linear scale. In some groups that have very close galaxy pairs  $R_{\text{vir}}$  may be very small  $\sim 10^{-3} - 10^{-4} h^{-1} \text{Mpc}$  and therefore  $\Delta/R_{\text{vir}}$  can have large values. We note that the values this small are not realistic, since the typical galaxy size is in order of 10kpc. This shows that in some cases (especially for groups with only a few members) the group  $R_{\text{vir}}$  is not the real virial radius.

The dashed lines in Fig. 8 show an uniform distribution of galaxies and all groups follow this curve up to  $\sim 1R_{\text{vir}}$ . After this point the observations and simulations start to notably deviate from the uniform galaxy distribution. In the observations there are remarkably less galaxies outside the virial radius at the outskirts of the groups. If close galaxy pairs are removed, the agreement outside the virial radius (as defined in this study) is much better, but in simulations there are still more galaxies in the outskirts of the groups than in the observations. The group richness does not have a notable effect on the distributions, since the upper panels and lower panels are qualitatively similar. By using another observational group catalogue and a different mock group catalogue, Snaith et al. (2011) noticed that SAMs produce radial distributions of galaxies which is more centrally concentrated than in the observations. Although our results and theirs are not directly comparable, we observe a similar small effect (upper left panel). The difference would be more evident if the distributions are normalised.

Lastly, we studied the spatial location of the most luminous galaxy in the group. For  $N_{\text{gal}} \geq 10$  groups, in observations the mean distance between the luminosity centre and the brightest galaxy is  $\sim 0.15 \pm 0.01 h^{-1} \text{Mpc}$  for the  $M \leq -18$  sample and  $\sim 0.52 \pm 0.10 h^{-1} \text{Mpc}$  for the  $M \leq -21$  sample. In simulations the mean distance is the same for the  $M \leq -18$  sample,  $\sim 0.13 \pm 0.01 h^{-1} \text{Mpc}$ , but notably smaller for the  $M \leq -21$  sample,  $\sim 0.15 \pm 0.01 h^{-1} \text{Mpc}$ . Also, mean luminosities of the brightest galaxies are systematically 2–5 times larger in the simulations compared with observations. Since the samples used in this analysis can be connected to the mean mass of the groups (see Table 4) we conclude that SAM used in this analysis produces too bright galaxies close to the centre of the groups in the massive galaxy groups.

In general, our galaxy distributions cannot be directly compared with other galaxy density distribution studies (e.g. Yang et al. 2005, Chen 2008, More et al. 2009). Our normalized galaxy density distribution is based on the statistically corrected 3-D positions and this makes the distribution more uniform than what it really is. Our distribution does not directly correspond the true galaxy density profile. Still, we can analyse the differences between the observed and SAM data that are processed in the same way.

One explanation for the observed difference may be due to physical processes influencing galaxy evolution that are not modelled correctly by SAMs. There are many processes that may influence the results at the outskirts of groups and cause the overabundance of galaxies. Although many physical processes are effective at the galaxy cluster scale, it has been shown that the same processes can be effective also in low-velocity dispersion systems (e.g., Zabludoff & Mulchaey 1998, Weinmann et al. 2006a). The ram pressure stripping (Gunn & Gott 1972), a cut-off of gas accretion onto galaxy discs by different processes (strangulation, Larson et

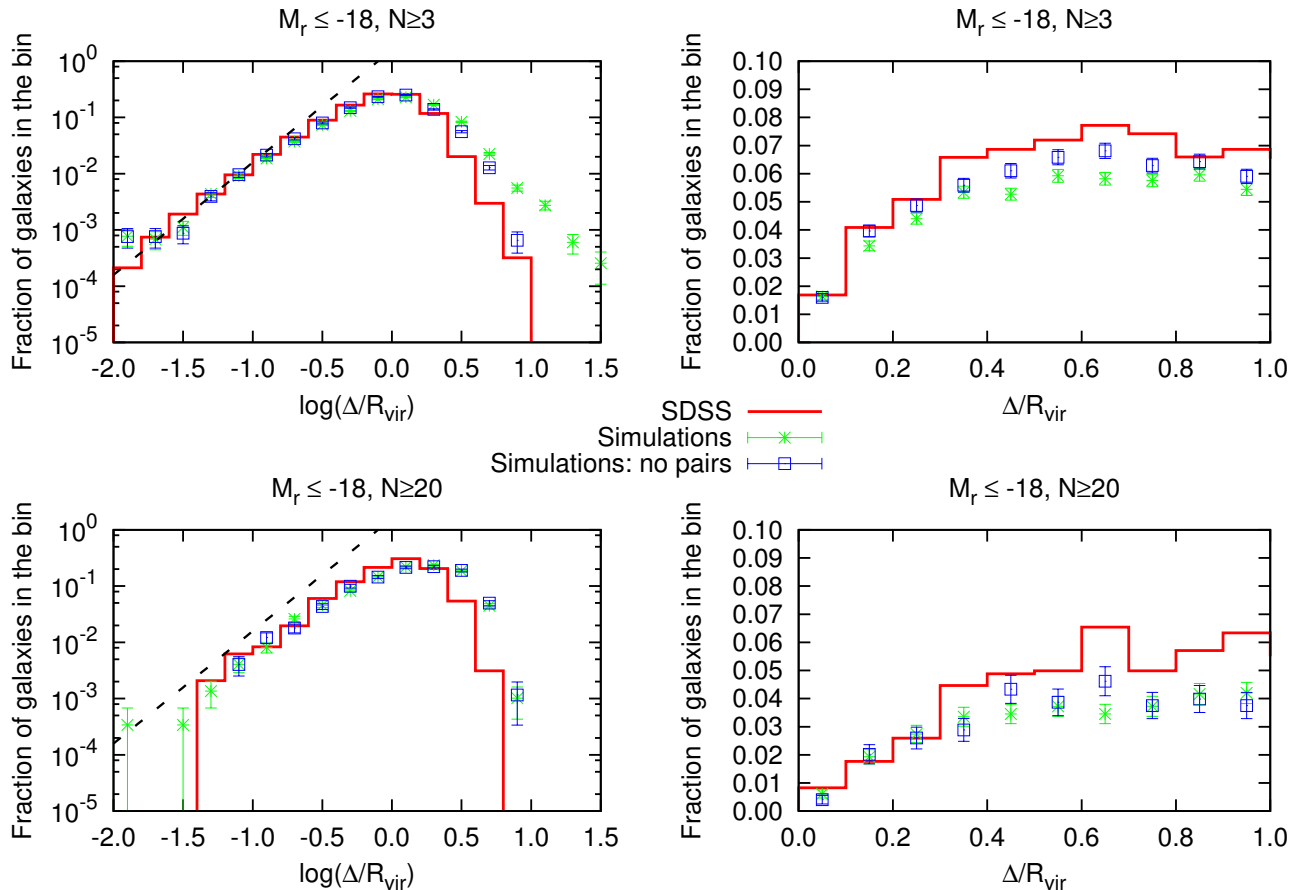


**Figure 8.** Radial number distribution of galaxies as a function of the normalised distance  $\Delta/R_{\text{vir}}$  from the luminosity centre. All galaxy groups are averaged together and scaled with respect to their virial radii. Black dashed lines show the distributions for the uniform spatial density of galaxies. The left panels show the distributions up to  $\Delta \sim 30R_{\text{vir}}$  and the right panels show only the inner regions of the groups. The upper panels are for groups with  $N \geq 3$  and the lower panels show only rich groups with  $N \geq 20$ . “No pairs”-data points are for the modified mock data (see Sec. 3.4).

al. 1980, Balogh, Navarro and Morris 2000, Croton et al. 2006) and high-velocity close encounters of satellite galaxies called harassment (Moore et al. 1996) are all examples of processes that can change the  $r$ -band luminosities of galaxies (visibility in the mock data) and therefore affect the shape of the distribution.

Differences between Durham and Munich SAMs are studied in detail by Contreras et al. (2013). They show that the Durham and Munich models produce a different spatial distribution of satellite galaxies within the main halo. The Durham satellite galaxies are more clustered at small scales while the spatial distribution of the resolved subhaloes is more extended in the Munich model. Moreover, the Munich model produces about three times more satellites with resolved subhaloes than the Durham one. Contreras et al. (2013) concluded that the reason for this is the difference between subhalo/satellite merger procedures in the Munich and Durham models.

## 4 CONCLUSION AND DISCUSSION

Although galaxy groups are the most common environment for galaxies, this very diverse population from loose associations of a few galaxies up to systems with several tens of galaxies is relatively poorly studied. An important result obtained in many studies is that physical properties of galaxies (colours etc.) are different in different types of groups (e.g. Yang et al. 2008, Weinmann et al. 2006a, Weinmann et al. 2006b, Mendel et al. 2011). Although DM drives the formation of the large-scale structure, the models of formation of galaxies are far from completely understood. This problem has been stressed by several authors and disagreements between the mock catalogues and observed catalogues have been reported. For example, Robotham et al. (2011) found a remarkable deficit in the number of observed high multiplicity groups compared to the mocks. They also found that there were significantly less compact groups in the observed data.

However, it should be remembered that the mock catalogues and the results derived from them are cosmology dependent. In Yang et al. (2005) and van den Bosch (2005) it was shown that a cosmology with  $\sigma_8 \sim 0.7$  gives better

agreement between simulations and observations for high multiplicity groups than  $\sigma_8 \sim 0.9$  used in MS. Using the rescaling technique of Angulo & White (2010), Guo et al. (2013) scaled MS based on WMAP1 cosmology (Bennett et al. 2003) to WMAP7 cosmology (Komatsu et al. 2011). They concluded that there is no considerable effect of different cosmologies for halo mass functions at least up to  $z = 3$ . The amplitude parameter  $\sigma_8$  is lower in the WMAP7 cosmology, but the matter density  $\Omega_m$  is higher for WMAP7. The net result is that these two effects cancel each other. They summarize, that different cosmologies (WMAP1 or WMAP7) produce only small differences in galaxy properties. In Guo et al. (2013) fig. 6, they show that their SAM (Munich model), updated for WMAP7 cosmology, slightly increases the abundance of luminous galaxies.

Observationally and physically the definition of a galaxy group is not trivial, since they represent a wide mass range of systems from individual galaxies and their satellites to large clusters of galaxies. There are many methods and algorithms to identify galaxy groups and clusters (e.g. Hugra & Geller 1982, Yang et al. 2005b, Tago et al. 2010) that have been used to extract different group catalogues. This makes it very complicated to compare the group properties in different catalogues in the same way and the group catalogues need to be studied separately. We have to also remember that observational galaxy catalogues are never ideal. Different observational constraints need to be taken into account and direct comparison may contain observational limitations. We have tried to eliminate some of these biases by using volume-limited galaxy samples. This allowed us to compare the number densities of the groups and to compare group properties directly with simulations.

In our study we compared the mock group catalogues with the SDSS group catalogues, both constructed by using the same algorithm. For the most part these two group catalogues agree well. First, our comparison showed that the richness distributions agree well between the simulations and SDSS. The numbers of pairs and loose groups match very well, but simulations give richer groups. Also the  $\sigma_v$  distributions are very similar, confirming the idea that the velocity distribution is not sensitive to the group definition. The rms velocity  $\sigma_v$  does not reflect efficiently the differences in the group properties. Clear discrepancies are seen in the group size and virial radius distributions. Also, there are clear differences in the spatial galaxy distributions. In simulations there are more galaxies beyond the virial radius than in the observations, if no modifications are done to the mock catalogue. The agreement is much better if we remove all close galaxy pairs from the mock catalogue, mimicking the observational bias. Also, different physical processes that are not modelled properly by SAM may play a role in this discrepancy. Another reason for this discrepancy might be the fact that the connection between the DM haloes and galaxies is not trivial. Some subhaloes may not have an observed counterpart as suggested by Gao et al. (2004a). Guo et al. (2011) also found that galaxy distributions in rich clusters agree between their simulations and observations only if galaxies without DM subhaloes (orphan galaxies) are included. This can be problematic in SAMs, where DM halo mergers and masses are followed during the simulations and galaxy modelling is based on the DM halo evolution.

Finally, to check how the overabundance of bright galax-

ies in the simulated catalogues affects our results, we removed all bright galaxies with  $M_r - 5 \log h \leq -22$  from the simulated data (see Fig. 1), produced all the mock group property distributions again and studied how the distributions differ from the original ones. The distributions were surprisingly similar with the original distributions and all the values in the histograms were within the error bars, except for the  $M_r \leq -21$  sample. Here marginal differences were seen and the agreement with the observations was slightly better, but all the conclusions and general results given in the paper are still valid, even if the brightest galaxies are totally excluded from the simulations.

The main results of this study are as follows:

(i) We have calculated the statistical properties of the SDSS-DR7 group catalogues. The results are listed in Tables 1, 2, 5–8.

(ii) In the Bertone SAM data the luminosity function of galaxies differs notably from observations for  $M_r - 5 \log h \leq -21.5$ , being biased towards higher luminosities.

(iii) For SDSS data the richness distributions follow simple power laws and the calculated logarithmic least-square slope values are  $-2.02 \pm 0.18$ ,  $-2.12 \pm 0.17$ ,  $-2.26 \pm 0.19$  and  $-3.29 \pm 0.24$  for  $M_r \leq -18$ ,  $-19$ ,  $-20$  and  $-21$ , respectively. SAM results from the Bertone and Font data give significantly different results from observations. There are too many rich and luminous groups in SAM data compared with observations.

(iv) The SDSS group catalogue includes incompleteness at small galaxy separations. This is especially important for galaxy pairs of small sizes. For  $\log R_{\max}[h^{-1} \text{Mpc}]$  these limitations start from  $-1.46$ ,  $-1.28$ ,  $-1.11$  and  $-0.0955$ , for the volume-limited samples  $M_r \leq -18$ ,  $M_r \leq -19$ ,  $M_r \leq -20$ ,  $M_r \leq -21$ , respectively, and grow for smaller sizes. Since  $R_{\text{vir}}$  and  $R_{\text{max}}$  are strongly correlated, the same limitation is a problem also for the  $R_{\text{vir}}$  distribution.

(v) For all samples the correlation between  $R_{\text{vir}}$  and the rms velocity  $\sigma$  is either weak or non-existent. Excluding galaxy pairs, in observations the group luminosity is weakly correlated with  $R_{\text{vir}}$ ,  $R_{\text{max}}$  and  $\sigma$ .

(vi) In the Tago et al. (2010) catalogue there are less galaxies at the outskirts of a group than in simulations. In the inner regions the galaxies have an almost uniform number density for all groups. The agreement is better if the observational galaxy pair bias is taken into account. However, this distribution does not correspond to the true galaxy density profile, since in our comparison we use a statistical 3-D radius that makes the distribution more uniform than it really is.

Summarizing, the comparison between the mock group catalogue and observations reveal interesting differences. Some of these differences are due to the problems in the properties of galaxies generated by semi-analytical methods (SAMs). Some differences can be associated with the observational limitations in the SDSS galaxy data. In future studies, we will analyse how tight is the connection between the underlying DM halo and the galaxy group. Do all observed groups have a main DM halo or are they in some cases just loose connections of separate DM haloes?

**ACKNOWLEDGEMENTS**

This study was supported by the Finnish Academy funding, the Turku University Foundation, the Estonian Science Foundation grants No. 8005, 7765, 9428 and MJD272, the Estonian Ministry for Education and Science research project SF0060067s08, and by the European Structural Funds grant for the Centre of Excellence "Dark Matter in (Astro)particle Physics and Cosmology" TK120. This work has also been supported by ICRAnet through a professorship for Jaan Einasto. We thank Chris Flynn and Sarah Bird for all valuable corrections and comments about the paper.

**REFERENCES**

- Allam S. S., Tucker D. L., 2000, *Astron. Nachr.*, 321, 101  
 Adelman-McCarthy J. K., et al., 2008, *ApJS*, 175, 297  
 Abazajian K. N., et al., 2009, *ApJS*, 182, 543  
 Angulo R. E., White S. D. M., 2010, *MNRAS*, 405, 143  
 Balogh M. L., Navarro J. F., Morris S. L., 2000, *ApJ*, 540, 113  
 Bennett C. L., et al. 2003, *ApJS*, 148, 1  
 Berlind A., et al., 2006, *ApJSS*, 167, 1  
 Bertone S., De Lucia G., Thomas P. A., 2007, *MNRAS*, 379, 1143  
 Blanton M. R., et al., 2003, *ApJ*, 592, 819  
 Blanton M. R., et al., 2005, *AJ*, 129, 2562  
 Binney&Tremaine, 1987, *Galactic Dynamics*. Princeton University Press, Princeton, NJ  
 Biviano A., Girardi M., 2003, *ApJ*, 585, 205  
 Bower R. G., Benson A. J., Malbon R., Helly J. C., Frenk C. S., Baugh C. M., Cole S., Lacey C. G., 2006, *MNRAS*, 370, 645  
 Boylan-Kolchin M., Springel V., White S. D. M., Jenkins A., Lemson G., 2009, *MNRAS*, 398, 1150  
 Bryan S. E., Mao S., Kay S. T., 2008, *MNRAS*, 391, 959  
 Carlberg R. G. et al., 1997, *ApJ*, 485, 13  
 Chen J., 2008, *A&A*, 484, 347  
 Cole S., Lacey C. G., Baugh C. M., Frenk C. S., 2000, *MNRAS*, 319, 168  
 Conroy C., Wechsler R. H., Kravtsov A. V., 2006, *ApJ* 647, 201  
 Contreras S., Baugh C. M., Norberg P., Padilla N., 2013, *MNRAS*.tmp.1272C  
 Coziol R., Andernach H., Caretta C. A., Alamo-Martínez K. A., Tago E., 2009, *AJ*, 137, 4795  
 Croton D. J., et al., 2006, *MNRAS*, 365, 11  
 De Lucia G., Springel V., White S. D. M., Croton D., Kauffmann G., 2006, *MNRAS*, 366, 499  
 De Lucia G., Blaizot J., 2007, *MNRAS*, 375, 2  
 Dressler A., 1980, *ApJ*, 236, 351  
 Eckmiller H. J., Hudson D. S., Reiprich T. H., 2011, *A&A*, 535, 105  
 Einasto J., Saar E., Kaasik A., Chernin A. D., 1974, *Nature*, 252, 111  
 Einasto M., Vennik J., Nurmi P., Tempel E., Ahvensalmi A., et al., 2012, *A&A*, 540, 123  
 Eke V. R., Baugh C. M., Cole Shaun, Frenk C. S., King H. M., Peacock, J. A., 2005, *MNRAS*, 362, 1233E  
 Ellison S. L., Patton D. R., Simard L., McConnachie A. W., 2008, *AJ*, 135, 1877  
 Ellison S. L., Patton D. R., Simard L., McConnachie A. W., Baldry I. K., Mendel J. T., 2010, *MNRAS*, 407, 1514  
 Font A. S., Bower R. G., McCarthy I. G., Benson A. J., Frenk C. S., Helly J. C., Lacey C. G., Baugh C. M., Cole S., 2008, *MNRAS*, 389, 1619  
 Huchra J. P., Geller M. J., 1982, *ApJ*, 257, 423  
 Gao L., White S. D. M., Jenkins A., Stoehr F., Springel V., 2004a, *MNRAS*, 355, 819  
 Gao L., De Lucia G., White S. D. M., Jenkins A., 2004b, *MNRAS*, 352, L1  
 Gunn J. E., Gott J. R. I., 1972, *ApJ*, 176, 1  
 Guo Q., White S., Boylan-Kolchin M., et al., 2011, *MNRAS*, 413, 101  
 Guo Q., Cole S., Eke V., Frenk C., Helly J., 2013, arXiv1301.3134G  
 Geller M. J., Huchra J. P., 1983, *ApJS*, 52, 61G  
 Jarosik N., et al., 2011, *ApJS*, 192, 14  
 Jenkins A., Frenk C. S., White S. D. M., Colberg J. M., Cole S., Evrard A. E., Couchman H. M. P., Yoshida N., 2001, *MNRAS*, 321, 372  
 Karachentsev I. D., 2005, *AJ*, 129, 178  
 Kim H. S., Baugh C. M., Cole S., Frenk C. S., Benson A. J., 2009, *MNRAS*, 400, 1527  
 Kimm T., Somerville R. S., Yi S. K., van den Bosch F. C., Salim S., Fontanot F., Monaco P., Mo H., Pasquali A., Rich R. M., Yang X., 2009, *MNRAS*, 394, 1131  
 Klypin A., Trujillo-Gomez S., Primack J., 2011, *ApJ*, 740, 102  
 Komatsu E. et al., 2011, *ApJS*, 192, 18  
 Larson R. B., Tinsley B. M., Caldwell C. N., 1980, *ApJ*, 237, 692  
 Liivamägi L. J., Tempel E., Saar E., 2012, *A&A*, 539, 80  
 Lin Y. T., Mohr J. J., Stanford S. A., 2004, *ApJ*, 610, 745  
 Liu L., Yang X., Mo H. J., van den Bosch F. C., Springel V., 2010, *ApJ*, 712, 734  
 Maller A. H., Katz N., Kereš D., Daé R., Weinberg D. H., 2006, *ApJ*, 647, 763  
 Mendel J. T., Ellison S. L., Simard L., Patton D. R., McConnachie A. W., 2011, *MNRAS*, 418, 1409  
 Moore B., Katz N., Lake G., Dressler A., Oemler A. 1996, *Nature*, 379, 613  
 More S., van den Bosch F. C., Cacciato M., Mo H. J., Yang X., Li R., 2009, *MNRAS*, 392, 801  
 Mulchaey J. S., 2000, *ARA&A*, 38, 289  
 Muñoz-Cuartas J.C., Müller V., 2012, *MNRAS*, 423, 1583  
 Niemi S.-M., et al., 2007, *MNRAS*, 382, 1864  
 Patton D. R., Ellison S. L., Simard L., McConnachie A. W., Mendel J. T., 2011, *MNRAS*, 412, 591  
 Planck Collaboration XVI, 2013, arXiv1303.5076  
 Potsman M., Geller M., 1984, *ApJ*, 281, 95  
 Press W. H., Schechter P., 1974, *ApJ*, 187, 452  
 Robotham A. S. G., Norberg P., Driver S. P., et al., 2011, *MNRAS*, doi:10.1111/j.1365-2966.2011.19217.x  
 Sheth R., Tormen G., 1999, *MNRAS*, 308, 119  
 Springel V., et al., 2005, *Nature*, 435, 629  
 Skibba R. A., van den Bosch F. C., Yang X., More S., Mo H. J., Fontanot F., 2011, *MNRAS*, 410, 417  
 Snaith O. N., Gibson B. K., Brook C. B., Courty S., Sánchez-Blázquez P., et al., 2011, *MNRAS*, 415, 2798  
 Strauss M. A., et al., 2002, *AJ*, 124, 1810  
 Sun M., Voit G. M., Donahue M., Jones C., Forman W., Vikhlinin A., 2009, *ApJ*, 693, 1142



- Tago E., Saar E., Tempel E., Einasto J., Einasto M., Nurmi P., Heinämäki P. 2010, *A&A*, 514, 102
- Tempel E., Saar E., Liivamägi L.J., Tamm A., Einasto M., Einasto J., Müller, V., 2011, *A&A*, 529, A53
- Tempel E., Tago E., Liivamägi L.J., 2012, *A&A*, 540, A106
- Tucker D. L., et al., 2000, *ApJS*, 130, 237
- van den Bosch F. C., Yang X., Mo H. J., Norberg P., 2005, *MNRAS*, 356, 1233
- van der Marel R. P., Magorrian J., Carlberg R. G., Yee H. K. C., Ellingson E., 2000, *AJ*, 119, 2038
- Weinberg D. H., Davé R., Katz N., Hernquist L., 2004, *ApJ*, 601, 1
- Weinmann S. M., van den Bosch F. C., Yang X., Mo H. J., 2006a, *MNRAS*, 366, 2
- Weinmann S. M., van den Bosch F. C., Yang X., Mo H. J., Croton D. J., Moore B., 2006b, *MNRAS*, 372, 1161
- Weinmann S. M., Kauffmann G., von der Linden A., De Lucia G., 2010, *MNRAS*, 406, 2249
- Wen et al., 2012, *ApJS*, 199, 34
- Yang X., Mo H. J., van den Bosch F. C., Jing Y. P., 2005, *MNRAS*, 356, 1293
- Yang X., Mo H. J., van den Bosch F. C., Weinmann S. M., Li C., Jing Y. P., 2005, *MNRAS*, 362, 711
- Yang X., Mo H. J., van den Bosch F. C., et al., 2007, *ApJ*, 671, 153
- Yang X., Mo H. J., van den Bosch F. C., 2008, *ApJ*, 676, 248
- Yang X., Mo H. J., van den Bosch F. C., 2009, *ApJ*, 695, 900
- York D. G., Adelman J., Anderson Jr., J. E., et al. 2000, *AJ*, 120, 1579
- Zabludoff A. I., Mulchaey J. S., 1998, *ApJ*, 496, 39